Terahertz spectroscopy for the study of paraffin-embedded gastric cancer samples

ARTICLE *in* JOURNAL OF MOLECULAR STRUCTURE · DECEMBER 2014

Impact Factor: 1.6 · DOI: 10.1016/j.molstruc.2014.09.002

Journal of Molecular Structure 1079 (2015) 391–395

Contents lists available at ScienceDirect

Journal of Molecular Structure

journal homepage: www.elsevier.com/locate/molstruc

Terahertz spectroscopy for the study of paraffin-embedded gastric cancer samples

Faustino Wahaia [a,*], Irmantas Kasalynas [b], Dalius Seliuta [b], Gediminas Molis [c], Andrzej Urbanowicz [c,d], Catia D. Carvalho Silva [e], Fatima Carneiro [e,f,g], Gintaras Valusis [b], Pedro L. Granja [a,h,i]

[a] INEB – Instituto de Engenharia Biomédica, Universidade do Porto, Porto, Portugal
[b] Terahertz Photonics Laboratory, Optoelectronics Department of the Center for Physical Sciences and Technology, Vilnius, Lithuania
[c] TERAVIL Ltd, Vilnius, Lithuania
[d] Center for Physical Sciences and Technology, Vilnius, Lithuania
[e] FMUP – Faculdade de Medicina, Universidade do Porto, Porto, Portugal
[f] IPATIMUP – Institute of Molecular Pathology and Immunology of the University of Porto, Porto, Portugal
[g] Centro Hospitalar São João, Porto, Portugal
[h] ICBAS – Instituto de Ciências Biomédicas Abel Salazar, Universidade do Porto, Porto, Portugal
[i] FEUP – Faculdade de Engenharia, Universidade do Porto, Porto, Portugal

HIGHLIGHTS

- Gastric cancer detection.
- Paraffin-embedded samples.
- Cancer affected tissue regions, low transmittance.
- High absorption coefficient and refractive index for affected tissue.
- Dehydration of bio-tissues lead *t* low contrast.

ARTICLE INFO

Article history:
Received 2 April 2014
Received in revised form 28 July 2014
Accepted 2 September 2014
Available online 10 September 2014

Keywords:
Gastric adenocarcinoma
Cancer staging
Benign and cancerous tumor
THz spectroscopy

ABSTRACT

Terahertz (THz) spectroscopy constitute promising technique for biomedical applications as a complementary and powerful tool for diseases screening specially for early cancer diagnostic. The THz radiation is not harmful to biological tissues. As increased blood supply in cancer-affected tissues and consequent local increase in tissue water content makes THz technology a potentially attractive. In the present work, samples of healthy and adenocarcinoma-affected gastric tissue were analyzed using transmission time-domain THz spectroscopy (THz-TDS). The work shows the capability of the technique to distinguish between normal and cancerous regions in dried and paraffin-embedded samples. Plots of absorption coefficient α and refractive index n of normal and cancer affected tissues, are presented and the conditions for discrimination between normal and affected tissues are discussed.

Introduction

Among the most common worldwide causes of cancer death is gastric cancer (with about 738,000 deaths per annum, 9.7% of all cancer cases) [1]. Early clinical diagnosis of gastric cancer is crucial for in time patients' treatment. Usually microscopic pathology is the most commonly used technique for tissue analysis. Embedding tumor bio-tissues in paraffin for histopathologic analysis is a widely used fixation method owing to its better storage and long-term tissue morphology preservation in clinical settings [2]. There are many other optical techniques being investigated for this purpose, and, the introduction of THz spectroscopy appears to be a powerful instrument to contribute for the solution of the important health and social problem associated with cancer. However, there are still many challenging issues to overcome such as better understanding of THz bio-interaction for THz spectroscopy and safety guidelines, which could enable the development of reliably powerful THz biomedical spectroscopy systems for further improvement of early cancer diagnosis. And are, thus, expected to bring a more comprehensive screening and diagnosis of human

* Corresponding author at: INEB – Instituto de Engenharia Biomédica, Universidade do Porto, Rua do Campo Alegre, 823, 4150-180 Porto, Portugal.
E-mail address: faustino.wahaia@ineb.up.pt (F. Wahaia).

http://dx.doi.org/10.1016/j.molstruc.2014.09.002
0022-2860/

disease, particularly in the case of gastric and other cancers. This technique are based on the specific spectroscopic fingerprints of biological medium in the THz spectral region [3].

The terahertz region lies between the microwave and infrared regions of the electromagnetic spectrum. It has very low photon energy – 1 THz is 4.1 MeV – and thus it does not pose any ionization hazard for biological tissues [4], and they have small dispersion and large absorption in the terahertz range [5]. THz radiation has a shorter wavelength than that of microwave frequencies enabling higher spatial resolution capabilities. The radiation is very sensitive to water content and strongly attenuated by water, non-ionizing, and power levels found in pulsed systems (<1 μW) are orders of magnitude lower than the maximum permissible beam power as determined by ionizing radiation safety guidelines [6]. Furthermore, owing to the coherent time gated detection technique there is an efficient elimination of background noise which commonly leads to a very high signal to noise ratio (>10,000:1 at 1 THz). Because of these characteristic properties, there has been growing interest in THz imaging and spectroscopy for biomedical application in recent years. In addition increasing studies are being reported using THz technology in spectroscopic studies of cancer [7,8]. The presence of cancer often causes increased blood supply in affected tissues and a local increase in tissue water content [9], fact acting as a natural contrast mechanism for THz imaging of cancer. Moreover, the structural changes that occur in affected tissues have also been shown to contribute to THz-TDS's spectra contrast [10,11].

Histo-pathologists use microscopic imaging methods of biopsied tissue parts to provide structural and functional information, X-ray imaging, magnetic resonance imaging MRI to provide images of living tissues at the macroscopic level, but at much lower resolution and specificity [12,13]. Alternative techniques of highly-resolved imaging for *in-vivo* diagnostic screening capable of providing early detection of disease are highly still desirable. THz imaging may constitute a powerful tool to complement these and other currently used techniques in years to come.

Terahertz spectroscopy provides broadband information on biosamples making it possible to distinguish between tissue regions with different optical characteristics (e.g., healthy and neoplastic tissue) over the reliable working THz frequency range. THz-TDS has previously been used to obtain the THz optical characteristics of skin tissue [11,14]. THz-TDS has also been used to successfully characterize DNA and proteins, allowing intermolecular interactions to be probed [15,16]. Because of the advantages listed above, THz techniques have the potential to become a particularly viable tool for early cancers diagnostic. First published results specially, in cancer tissue imaging using THz pulsed radiation, suggest that THz imaging can be used for macroscopic visualization of tumor margins in fresh tissues [17–20], which was later confirmed by other studies on various cancer types and organs [21–23] and to identify contrast between healthy breast tissue and breast cancer [23]. It has been suggested that this technique could be used to assist surgeons performing breast-conserving surgery when excising tumor margins.

The present work is aimed at, firstly demonstrating the capability of THz-TDS for gastric cancer diagnosis and, secondly, exploring the technique's capability as a confirmatory (auxiliary) technique for early gastric cancer detection by distinguishing healthy tissue from the neoplastic one. The novelty of the present research work resides in (i) being the first study available concerning the application of THz-TDS for gastric cancer, (ii) showing that additional contrast-contributing factors other than water influence the diagnostic potential of this technique [24]. In more general terms, the present study intends to contribute to widen opportunities for THz science in medicine by the spatial resolution and data acquisition rate and by providing a better understanding of THz pulse propagation through complex media with the overall aim of developing cost effective and reliable diagnostic THz devices with endoscopic ability to provide access to internal epithelial surfaces for early cancer detection within the established safety guidelines.

Theoretical background: Samples' parameters extraction

Several authors presented material parameter extraction algorithms to determine the complex refractive indexes of samples with THz-TDS [25,26]. For that purpose, a THz pulse propagating through a sample is compared to another THz pulse propagating without the sample in its path. This is achieved by tracing the temporal shape of the electric field with sample $E_{sample}(t)$ and without sample $E_{ref}(t)$ where t is the optical delay time. These two pulses are transformed into the frequency domain using fast Fourier Transform to obtain the complex transmission spectra for the signal (sample embedded in paraffin) $E_{sample}(\omega)$, and for the reference (paraffin only), $E_{ref}(\omega)$. Considering normal incidence, the ratio of these fields is related to the absorption coefficient $\alpha(\omega)$ and refractive index $n(\omega)$ of the sample as follow [25–28],

$$\frac{E_{sample}(\omega)}{E_{ref}(\omega) = 4n(1+n)^{-2}e^{\frac{-k\omega d}{c(n-1)}}} = A(\omega)e^{-k\varphi(\omega)} \quad (1.1)$$

where ω, is the frequency, c, the speed of light in vacuum, d is the thickness of the sample, $A(\omega)$ is the amplitude ratio between the spectrum of the sample signal and that of the reference, and $\varphi(\omega)$ is the relative phase difference.

From the expression (1.1), refractive index and the absorption coefficient can be calculated through the following expressions [25,26,21–24]

$$n_{sample}(\omega) = 1 + (2\pi\omega d)^{-1}c\varphi(\omega) \quad (1.2)$$

$$\alpha_{sample}(\omega) = -2d^{-1}\ln\{[4n_{Sample}(\omega)]^{-1}A(\omega)[1+n_{sample}(\omega)]^2\} \quad (1.3)$$

Materials and methods

Experimental set-up

In this work, a Teravil-Ekspla T-Spec THz TDS system (Vilnius, Lithuania) was used in the frequency range 0.1–3.5 THz with a spectral resolution of <10 GHz. The layout of the system is shown in Fig. 1.

A photoconductive antenna made from GaBiAs, illuminated by ultra-short laser pulses, is used for THz radiation and detection. The antenna is formed using AuGeNi metallization. The fiber-based pumping laser provide pulses of 1064 nm wavelength, 150 fs pulse duration and 40 mW output power at 30 MHz pulse repetition rate. For more efficient collimation and focusing of THz radiation, a hemispherical lens fabricated from high resistance silicon is attached to the backside of the THz antenna. The fiber-based pumping laser has two outputs where, one part of the laser beam is used for illumination of THz emitter, the second part of laser beam is fiber coupled and is used to illuminate the THz detector and the other part goes through slow delay line and guided to the fast delay line. After the delay line the beam is guided to the THz emitter, where is focused to the gap of the photoconductive antenna. The second part of the beam goes to the THz detector. The generated sub-picosecond pulses of THz radiation are focused to the sample by parabolic mirror M2. The transmitted radiation from the sample is collected by the parabolic mirror M3, and then, registered by a fiber coupled THz detector after which the THz signal goes to a digital signal processing unit. By scanning fast optical delay line in 10 Hz frequency, the waveform of electrical field of THz radiation is build and a numerical Fourier transform operation

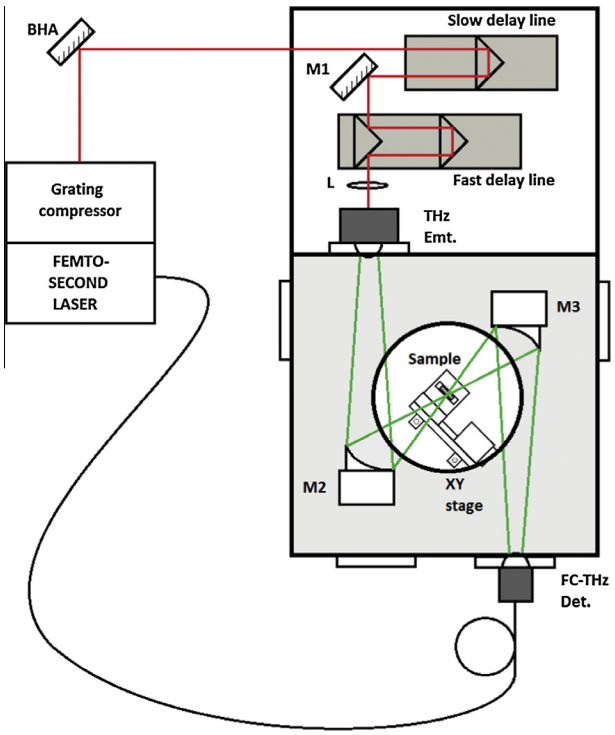

Fig. 1. Schematic set-up of optical components used in the THz-TDS system.

gives a spectral content of THz radiation. A comparison of the spectra with and without sample placed into the THz spectrometer's beam path gives the absorption and phase spectra of the samples under study. With the tissue sample placed in the THz beam path of the spectrometer, the signal to noise ratio is ~750:1, in fact related on the absorption coefficient and the thickness of the sample.

Sample preparation

A set of 21 paraffin-embedded blocks (samples) of gastric tissue were obtained from the archives of the Department of Pathologic Anatomy of Hospital São João Hospital (Porto, Portugal). All procedures using biological samples were performed and approved by the Ethics Committee of Centro Hospitalar S. João (CES 211-13 EPE).

Histological samples with constant thickness (2 mm), were taken from partial distal and total gastrostomy, and were of two types, namely (i) 11 adenocarcinoma pT3 (tumor invades subserosa or into non-peritonealized pericolic or perirectal tissues [29,30]) and, (ii) 10 pT4 (Tumor perforates visceral peritoneum and/or directly invades other organs or structures. In pT4a, the tumor perforates visceral peritoneum and, in pT4b, the tumor directly invades other organs or structures [29,30]). All of them analyzed under the same environmental conditions.

The samples were prepared according to standard histo-pathological procedures [31] for their fixation and paraffin embedding and mounting in plastic frames. Previous measurements of paraffin slices have shown that it has almost the same refractive index (n_{pfn} = 1.45) as high density polyethylene [32], n_{HDP} = 1.5 for the range of the working frequencies (0.25–1.00 THz).

Results and discussion

The terahertz radiation has been focused on the samples and the transmitted signal has been recorded. Fourier transformation was performed on the THz time signals, and the refractive indices and absorption coefficient have been calculated. Owing to the typical single-cycle nature of the THz pulse, its frequency spectrum extends from the low GHz region to several THz. At high frequencies the spectrum is characterized by a gradual roll-off, until the detected signal level approaches that of the noise floor of the experiment. The noise floor is normally independent of frequency and corresponds to the spectrum recorded with a completely blocked THz beam path. The origin of this noise is of an electronic nature, whereas fluctuations of the THz signal itself are caused, mainly by laser intensity fluctuations. A working frequency range from 0.25 to 1 THz was used in the measurements of the present work. Below 0.25 THz (lower limit), the electronics and laser pump fluctuations caused noise and lack of resolution, and above 1 THz (upper limit), strong noise associated to higher frequencies and noise of atmospheric absorption nature might have led to a very poor resolution, owing to that our reliable working frequency range has been in the interval from 0.25 to 1 THz.

Contrast on the spectra in Fig. 3 and 4, differences despite very faint owing to a very low THz contrast in waterless bio-tissues, not only between tumor and healthy tissues but also within tumors are noticeable. The refractive indices of the cancer affected tissue in each sample are higher than that of the healthy one. Actually, the refractive index is larger in the affected tissue for both, pT3 and pT4 tumors cases. In the pT4 case the difference is stronger albeit the spectra contrast on dehydrated biological tissues is known to be minimal.

As shown in Fig. 2, time-domain waveforms of healthy tissue and the two different tumors (1 and 2) can be seen. Here the **blue line** represents the healthy tissue, the **green** and **red lines** represent tumors 1 and 2 respectively. The reduction in amplitude is attributed mainly to the absorption during the beam transmission through the sample and the reflective losses. The delay in time arises from the different refractive indices of the different sample layers. Taking into account that the paraffin is transparent in the working frequencies, losses due to this medium were considered to be negligible.

Fig. 3 presents averaged THz amplitude transmittance waveforms for pT3 and pT4. Fig. 4 presents the average plots of calculated refractive index (n) and absorption coefficient (α) for pT3 and pT4 and the healthy tissue. All absorption features are accompanied by a characteristic change of the refractive index. Comparing the n and α spectra of the two types of tumors, that for pT3 has less contrast than that for pT4. The small differences, (i.e., the reduced contrast) between the two pathologic stages, pT3 and pT4, and the healthy tissue could be explained by the absence of water in the samples, that in freshly excised bio-tissue (where water is present with an absorption known to be around 170 cm^{-1} at 0.5 THz [33]) increases the contrast considerably [7,24].

Previous work exploring THz cancer diagnostics freshly excised tissues [22,23,34] reported differences on the refractive indices and absorption coefficients of cancer affected samples when compared to healthy tissue, which have been mainly attributed to the presence of higher water in the tumors [18,30]. However, other possible factors have been pointed out and additional studies have been suggested in order to better explain the effectiveness of THz radiation in cancer detection [4]. In the present work we also observe and confirm the existence of other contrast contributing factors, which could be the density of the affected tissue, the conditions within the tumor microenvironment (which differ considerably from those of normal tissue [35,36]), the rapid and uncontrolled cell division leading to an increased cell density and/or to the presence of certain proteins [37,38]. And that associated with the differences caused by cell alterations and abnormal protein density alterations, such the increase in the vascularization around tumors

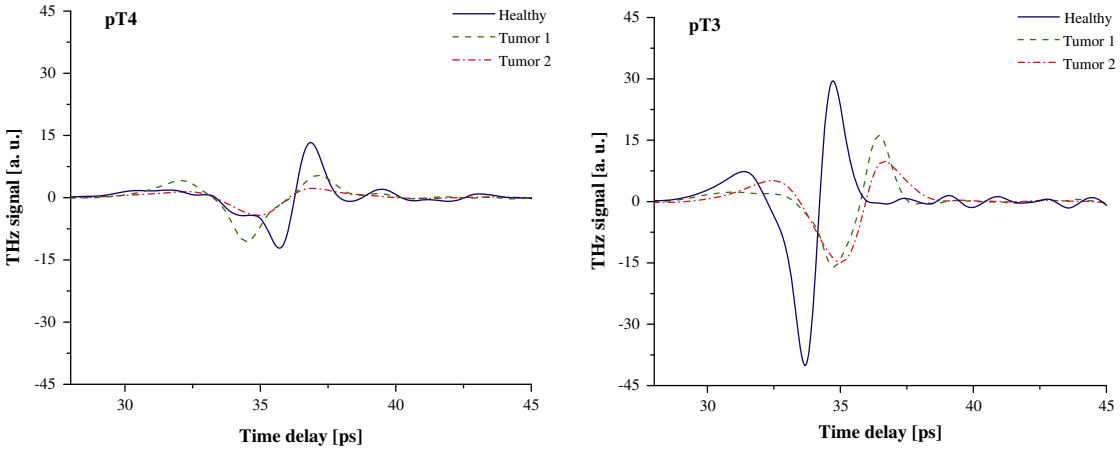

Fig. 2. THz spectroscopy on gastric tissue with adenocarcinoma pT3 and pT4. THz time-domain waveforms corresponding to healthy tissue and tissues with tumors 1 and 2.

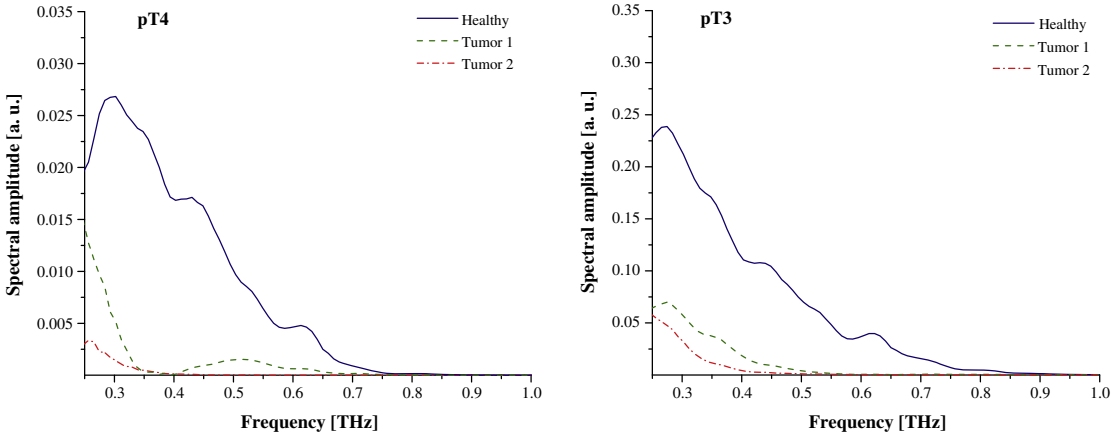

Fig. 3. Amplitude transmittance spectra for healthy tissue and tissues with tumors 1 and 2.

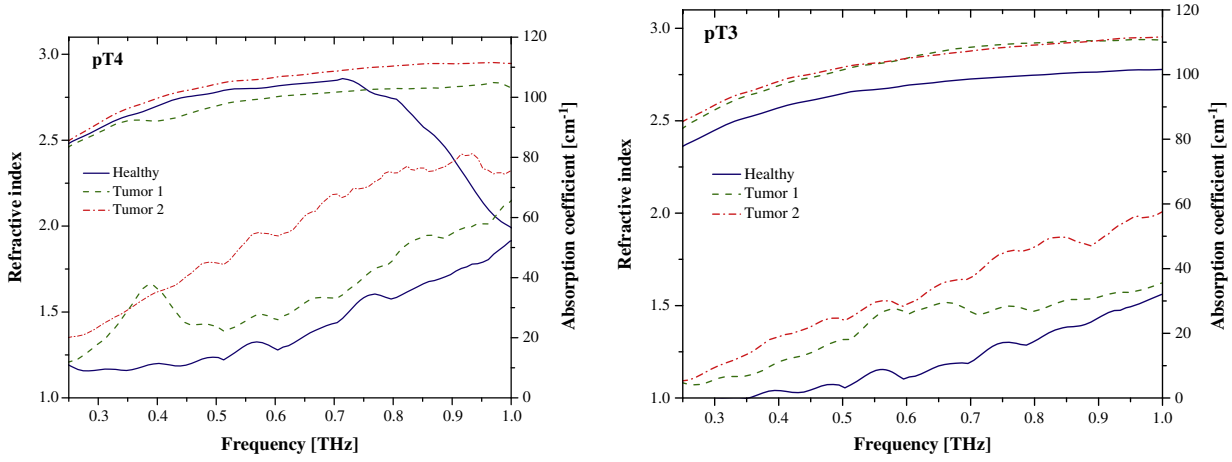

Fig. 4. Spectra of the absorption coefficients and the indices of healthy and tumors 1 and 2 tissues.

and consequent release of growth factors which in turn also lead to rapid cell division and higher cell densities [19]. The present results demonstrate the relevance of other factors, besides the water, although, as mentioned before, the contrast between healthy and tumor-affected tissues in dehydrated samples is too low and there is a need of contrast agents for better distinguishability.

Conclusions

We have studied a set of paraffin-embedded gastric tissue samples. The specimens have been taken from a tissue with the same bio-structural typology. Using THz time domain spectroscopy we have shown that cancer affected regions of all samples show higher refractive indices and absorption coefficients distinguishing them

from the adjacent healthy ones. The present study reinforces the feasibility of THz-TDS for gastric cancer detection. It also demonstrates that the characteristic higher percentage of water in cancerous tissues is not the single factor contributing to the contrast of the observed refractive index and the absorption coefficient.

Acknowledgements

The authors gratefully acknowledge financial support for this work from Science a Technology Foundation of Portugal (FCT) – SFRH/BPD/51470/2011, the Research Council of Lithuania under the "HeTeFo" project, contract No. MIP-093/2012, and from the BM1205 COST Action, for Short Term Scientific Mission of research Grant.

References

[1] J. Ferlay, H.-R. Shin, F. Bray, D. Forman, C. Mathers, D.M. Parkin, Int. J. Cancer 127 (12) (2010) 2893–2917, http://dx.doi.org/10.1002/ijc.25516.
[2] M. Doleshal, A.A. Magotra, B. Choudhury, B.D. Cannon, E. Labourier, A.E. Szafranska, J. Mol. Diagn. 10 (3) (2008) 203–211, http://dx.doi.org/10.2353/jmoldx.2008.070153.
[3] M.M. Nazarov, Quantum Electron. 38 (7) (2008) 647–654, http://dx.doi.org/10.1070/QE2008v038n07ABEH013851.
[4] L.V. Titova, A.K. Ayesheshim, A. Golubov, et al., Sci. Rep. 3 (2013) 2363, http://dx.doi.org/10.1038/srep02363.
[5] A.J. Fitzgerald, E. Berry, N.N. Zinov'ev, et al., J. Biol. Phys. 29 (2–3) (2003) 123–128, http://dx.doi.org/10.1023/A:1024428406218.
[6] IAEA Safety Standards Series, Safety Guide No. RS-G-1.1, Occupational Radiation Protection, International Atomic Energy Agency, 1999.
[7] Calvin Yu, Shuting Fan, Yiwen Sun, E. Pickwell-MacPherson, Quant. Imag. Med. Surg. 2 (1) (2012).
[8] E. Pickwell-macpherson, Terahertz Sci. Technol. 3 (4) (2010) 163–171.
[9] G.M. Png, J.W. Choi, B. Ng, S.P. Mickan, D. Abbott, Phys. Med. Biol. 53 (2008) 3501–3517.
[10] E.P. MacPherson, A.J. Fitzgerald, P.F. Taday, et al., Biol. Med. Appl. (2004) 821–822.
[11] V.P. Wallace, A.J. Fitzgerald, E.P. MacPherson, R.J.P.P.F. Taday, N. Flanagan, T. Ha, Appl. Spectrosc. 60 (10) (2006) 1127–1133.
[12] T. Loffler, T. Bauer, K.J. Siebert, H.G. Roskos, Opt. Express 9 (12) (2001) 616–621.
[13] Lei He, L. Rodney Long, Comput. Method Program Biomed. 107 (3) (2012) 538–556.
[14] S.Y. Huang, Y. Wang, D. Yeung, A.T. Ahuja, Y.T. Zhang, E.P. MacPherson, Phys. Med. Biol. 54 (2009) 149–160.
[15] J. Xu, T. Yuan, S. Mickan, X.-C. Zhang, Chines Phys Lett. 20 (8) (2003) 1266–1268.
[16] E.P.J. Parrott, Y. Sun, E. Pickwell-MacPherson, J. Mol. Struct. 1006 (1–3) (2011) 66–76, http://dx.doi.org/10.1016/j.molstruc.2011.05.048.
[17] R.M. Woodward, V.P. Wallace, D.D. Arnone, E.H. Linfield, M. Pepper, J. Biol. Phys. 29 (2003) 257–261.
[18] R.M. Woodward, B.E. Cole, V.P. Wallace, R.J.P.D.D. Arnone, E.H. Linfield, M. Pepper, Phys. Med. Biol. 47 (2002) 3853–3863.
[19] E. Pickwell, B. Cole, A.J. Fitzgerald, M. Papper, Phys. Med. Biol. 49 (2004) 1595–1607.
[20] E.P. MacPherson, V.P. Wallace, A.J. Fitzgerald, B.E. Cole, R.J. Pye, T. Ha, J. Biomed. Opt. 10 (2005) 64021.
[21] V. Wallace, A.J. Fitzgerald, E. Pickwell, R.J. Pye, P.F. Taday, Appl. Spectrosc. 60 (10) (2006) 1127–1133.
[22] A.J. Fitzgerald, V.P. Wallace, M. Jimenez-Linan, et al., Radiology 239 (2) (2006) 533–540.
[23] P.C. Ashworth, E.P. MacPherson, E. Provenzano, Opt. Express 17 (15) (2009) 12444–12453.
[24] F. Wahaia, Gintaras Valusis, Abílio Almeida, Joaquim A. Moreira, Irmantas Kasalynas, Dalius Seliuta, Ramunas Adomavicius, Jan Macutkevic, Patricia C. Lopes, M.L. Rui Henrique, L.M. Bernardo, J. Mol. Struct. 1006 (2011) 77–82.
[25] Lionel Duvillaret, Frédéric Garet, J.L. Coutaz, IEEE J. Sel. Topics Quantum Elect. 2 (3) (1996).
[26] A. Nahata, A.S. Weling, T.F. Heinz, Appl. Phys. Lett. 69 (16) (1996) 2321–2323.
[27] H. Ying, P. Huang, L. Guo, Wang, C. Zhang, Phys. Lett. 359 (2006) 728–732.
[28] Mingxia He, Meng Li, Weili Zhang, Piers Proc. (2008) 274–277.
[29] Leslie H. Sobin, Mary K. Gospodarowicz, Christian Wittekind, in: TNM Classification of Malignant Tumours, seventh ed., Wiley, 2014. <http://eu.wiley.com/WileyCDA/WileyTitle/productCd-1444332414.html>.
[30] AJCC Cancer Staging Manual. <http://www.springer.com/medicine/surgery/book/978-0-387-88440-0>, (25.07.14).
[31] M.J. Day, M.D. Willard, E.J. Hall, et al., J. Veter. Internal Med. (2010) 10–26.
[32] R. Piesiewicz, C. Jansen, S. Wietzke, D. Mittliman, M. Koch, T. Kurner, Int. J. Infrared. Milli. Waves (2007) 1–9.
[33] P.H. Siegel, IEEE Trans. Microw. Theory Tech. 52 (10) (2004) 2438–2447, http://dx.doi.org/10.1109/TMTT.2004.835916.
[34] T. Masahiko, M. Herrmann, K. Sakai, Meas. Sci. Technol. 13 (2002) 1739–1745.
[35] O.P. Cherkasova, M.M. Nazarov, A.P. Shkurinov, Radiophys. Quantum Electron. 52 (7) (2009) 518–523.
[36] T.Y. Reynolds, S. Rockwell, P.M. Glazer, Cancer Res. 56 (1996) 5754–5757.
[37] G.I. Mclntyre, Med. Hypothesis 66 (2006) 518–526.
[38] G.I. Mcltyre, Med. Hypothesis 69 (2007) 1127–1130.